International Journal of Mining, Reclamation and Environment

ISSN: (Print) (Online) Journal homepage: https://www.tandfonline.com/loi/nsme20

A COMPARATIVE STUDY ON POWER CALCULATION METHODS FOR CONVEYOR BELTS IN MINING INDUSTRY

Ekin Köken, Abiodun Ismail Lawal, Moshood Onifade & Ahmet Özarslan

To cite this article: Ekin Köken, Abiodun Ismail Lawal, Moshood Onifade & Ahmet Özarslan (2022) A COMPARATIVE STUDY ON POWER CALCULATION METHODS FOR CONVEYOR BELTS IN MINING INDUSTRY, International Journal of Mining, Reclamation and Environment, 36:1, 26-45, DOI: 10.1080/17480930.2021.1949859

To link to this article: https://doi.org/10.1080/17480930.2021.1949859

INTERNATIONAL JOURNAL OF MINING, RECLAMATION AND ENVIRONMENT
2022, VOL. 36, NO. 1, 26–45
https://doi.org/10.1080/17480930.2021.1949859

Taylor & Francis
Taylor & Francis Group

A COMPARATIVE STUDY ON POWER CALCULATION METHODS FOR CONVEYOR BELTS IN MINING INDUSTRY

Ekin Köken[a], Abiodun Ismail Lawal[b], Moshood Onifade[c] and Ahmet Özarslan[d]

[a]Abdullah Gul University, Department of Nanotechnology Engineering, Kayseri, Turkey; [b]Federal University of Technology, Department of Mining Engineering, Akure, Nigeria; [c]University of Nambia, Department of Civil and Mining Engineering, Ongwediva, Nambia; [d]Zonguldak Bulent Ecevit University, Department of Mining Engineering, Zonguldak, Turkey

ABSTRACT

This paper covers different methods to evaluate the power consumption of several conveyor belt systems (CBSs) used in the Turkish Mining Industry (TMI). Based on each CBS's operational features, the power consumption (P_c, kW) was measured directly on motorised head-pulleys. The P_c was investigated through several conventional, statistical, and machine learning methods. This study shows that the DIN 22,101 could be the most convenient conventional method for the investigated CBSs. On the other hand, based on the nonlinear regression (NLR) and genetic expression programming (GEP) models, two new approaches were suggested for the design and optimisation of the P_c.

ARTICLE HISTORY
Received 28 October 2020
Accepted 18 May 2021

KEYWORDS
Conveyor belt; mining; power calculation; regression algorithms; gene expression programming

1. Introduction

Conveyor belt systems (CBSs) are of prime importance in handling a wide range of bulk materials from metre to millimetre scale. According to [1], there are 2.5 million CBSs annually operating across the globe. Specific to the mining industry, CBSs have several advantages: higher capacity, lower cost, higher efficiency, and less human involvement than other bulk haulage systems such as trucking and conveyance by railway [2–9].

Following the rapid increase in measurement and visualisation techniques, different sensors, probes, high-speed cameras, and various measuring instruments have been integrated into CBSs for dynamic control of labour safety, monitoring belt tears, dust reduction, and determination of the particle size distribution of conveyed material [10–18]. In addition, CBSs with varying inclinations can be easily oriented to mobile crushers, which is very practical and beneficial for deep open-pit mines [19].

Owing to the applications mentioned herein, the use of CBSs has been inevitable for coal preparation, ore dressing, and crushing – screening plants. Therefore, CBSs should be continuously used during its service life and also work with optimum energy consumption.

In general terms, the power consumption of any conveyor belt is directly associated with the throughput, operating time, and efficiency of components embedded in the CBS infrastructure. These variables typically constitute a solid basis for evaluating the power draw of any CBS. More profoundly, the power consumption of CBSs is a critical factor in terms of both engineering economics and sustainable material transportation, where several factors should be investigated elaborately. Based on modern material transportation science and technology, the power consumption of CBSs can be handled by four different stages, namely: the equipment, operation, technology,

CONTACT Ekin Köken ekin.koken@agu.edu.tr

and performance indicators, each of which has typical qualifications [20,21]. The equipment indicators (EI) of CBS directly associates with operating components suitable in quality and dimension. For instance, bearings, shafts, gearboxes, and idlers with unsuitable quality and dimension can intensify the friction forces acting on belt surfaces.

The selection of head pulleys (e.g. bare, fully, or partially lagging ones) is another parameter that should be considered in the EI evaluations. If pulley selection is conducted in haste, a conveyor pulley may be inadequately sized and located, leading to premature pulley failure and costly downtime [22]. Belt tears or sags can also be observed when using low-quality belt materials or having difficulties in their installation. It should be herein mentioned that the size, density, and abrasivity of the conveyed material are the essential factors in selecting the belt material. For the last 25 years, the strength of belt materials has been reinforced using fabric carcases that determine the dynamic behaviour of CBSs [23]. For harsh environmental conditions, the belt rupture problem has also been solved by placing steel cords among the belt covers that improve the belt tensile strength [6]. When it comes to the performance of idlers, ambient temperature, humidity, and dust also have remarkable influences on power consumption [24].

The operation indicator (OI) of CBSs depends on the installation, adjustment, modification, and coordination of operating components and subsystems [25]. The most common variables for OI are the location of motorised pulley, throughput, belt speed, spacing of idlers, brake, start-stop, and take-up systems [26–31]. The design characteristics of CBS (e.g. belt length, slope, speed, etc.) can also be regarded in the context of OI. Although most CBSs are designed to meet the peak material flow (maximum throughput), they often run below their designed capacity. Practical experiences have demonstrated that CBSs should utilise 80–90% of motor nameplate horsepower to maximise motor life as a relative OI. As mentioned previously, belt sags are the other phenomena affecting power consumption. The Conveyor Equipment Manufacturers Association (CEMA) has declared that the optimal belt sag for CBSs should be within the limits of 1.5–3% [32]. Below this limit, tracking problems will be encountered due to the absence of friction between the belt and idlers. In addition to the tracking problems, excessive friction forces will be generated when going over the proposed limit.

According to Yao and Zhang [33], the overheating problems in motorised head-pulleys could be minimised by implementing multi-drives rather than single ones in the OI of CBSs. On the other hand, at the tail sections of CBSs, components or subsystems can be contaminated or buried by spilled materials, leading to a temporal or permanent shutdown. To eradicate such problems, modern belt cleaners have been developed [34,35].

The technological indicators (TI) of CBS incorporates all kinds of advances in components, mechanisms, and techniques that focus on the conservation, control, and diagnosis of individual subsystems, diminishing the friction, extending maintenance intervals, and optimising the energy consumption. The study by Blazej et al. [36] introduced a magnetic module of a control system called 'Diagbelt' for steel cord belts to reduce power consumption. Based on the fuzzy logic methodology, Ristić et al. [37] and Pang et al. [38] presented some speed control methodologies for some CBSs. Nevertheless, Petru and Mazen [39] pointed out that the performance of CBSs could also be improved by utilising pulse width modulation (PWM) techniques. In addition, He et al. [40] proposed another speed control methodology, considering the minimum speed requirements.

Adopting the three mentioned indicators (EI, OI, and TI), the performance indicator (PI) targets the maximisation of relevant process/product with minimum cost and emission. The PI focuses on minimising problems of CBSs under working conditions. It has been long experienced that the most critical problems affecting the functionality of CBSs are the overheat of motorised head pulley, belt sags, and tears. These problems are mainly caused by insufficient engine power, overloading, jams in/around the CBS elements, unsuitable belt speed, and damaged components (e.g. frames, belts, idlers, etc.). These problems impair CBS's effectiveness, sustainability, and stability and, therefore, lead to increased power consumption. The four indicators mentioned herein disclose the main reasons and possible solution pathways for optimising power consumption in most CBSs.

Considering these indicators, power consumption in any CBS can be arranged or regulated for sustainable material transportation.

Based on the framework of the mentioned four indicators, this study investigated the power consumption (P_c, kW) of several CBSs in Turkey using different methods. Firstly, the actual P_c of the investigated CBSs was measured directly on motorised head-pulleys. During the measurements, quantitative data on operational features were collected for each CBS. Based on the data available, the P_c was calculated with several conventional methods and also predicted using multiple linear regression (MLR), nonlinear regression (NLR), and gene expression programming (GEP) methods. The P_c values obtained from the mentioned methods were then discussed and compared with one another.

2. Summary of conventional power calculation methods for conveyor belts

For the calculation of P_c, the methods of CEMA (5th edition; $CEMA_5$ [32] and 7th edition: $CEMA_7$ [41]), DIN 22,101 [42] Dunlop–Fenner [43] was adopted in this study. Based on the collected data, the P_c was calculated for each CBS, considering the following methodologies.

2.1. CEMA methods

The CEMA has published seven editions of the guide entitled *'Belt conveyors for bulk materials'* since 1966. The first five editions ($CEMA_{1-5}$) of the guide follow the same procedures to calculate the P_c with minor revisions. For the last two editions ($CEMA_{6,7}$), several modifications in several formulae and new input parameters like idler conditions, start-stop, maintenance, and derating factors were integrated into the calculations. The common variables used in calculating the P_c are illustrated in Figure 1.

Based on the $CEMA_5$ [32], the calculation methodology of P_c was summarised as the SI (metric) unit system and given by the following equation systems:

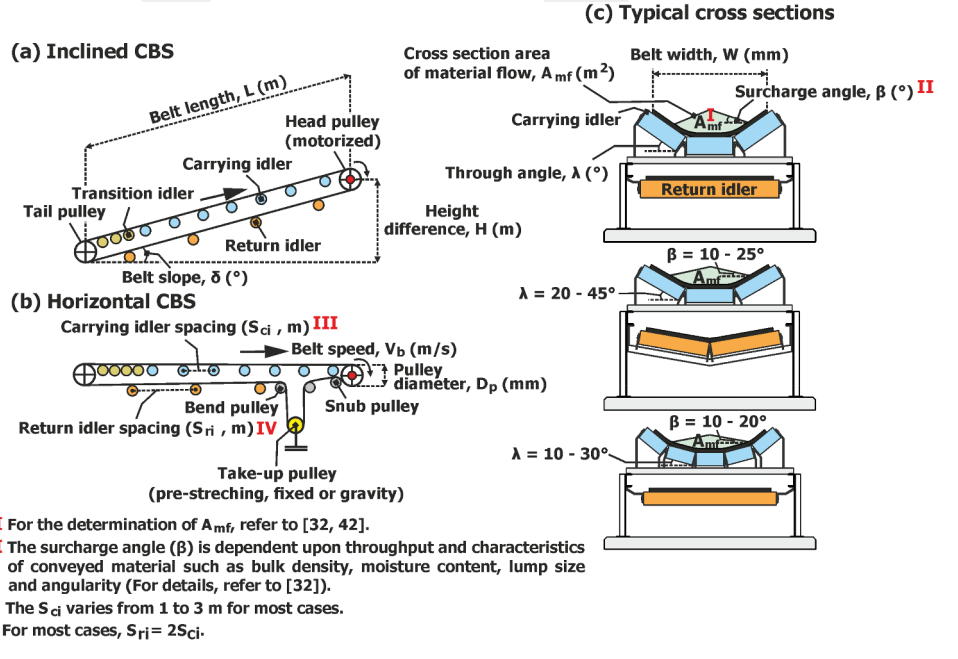

Figure 1. Schematic illustration and terminology of CBSs a) An inclined CBS b) A horizontal CBS c) Typical cross-sections of common CBSs (Modified after [44]).

$$P_c = T_b \times V_b \tag{1}$$

where T_b is the effective belt tension (kN) (Eq. 2), and V_b is the belt speed (m/s). P_c is kW in unit.

$$T_b = L \times K_t \times \left(K_x + W_b \times g \times \left(K_y + 0.015\right)\right) + W_m \times g \times \left(L \times K_y \pm H\right) + T_{p_e} + T_{am} + T_{ac} \tag{2}$$

where L is belt length (m), K_t is the ambient temperature correction factor (K_t = 1 at 20°C), K_x is the friction force (N/m) depending on idlers (Eq. 3). K_y is the constant based on the L and δ of the belt (Table 1). The g is the gravitational acceleration (9.81 m/s^2).

The W_b and W_m define the length-related weight (kg/m) of the belt and material (Eqs. 4,5), respectively. The H is the height difference (m) along with the CBS. T_{pe} is the effective resistance force on pulleys (N) (Table 2). The T_{am} is the force (N) required to accelerate the material on the CBS (Eq. 6), and T_{ac} is the resistance force of other accessories (N) (Eq. 7).

$$K_x = 0.00068 \times g \times (W_b + W_m) + \frac{A_i}{S_{ci}} \tag{3}$$

where A_i is the resistance forces (N) to rotate idlers (Based on the idler type, A_i = 3–9 N, $Cema_5$ [32

$$W_m = \frac{Q}{3.6 \times V_b} \tag{4}$$

where Q is the throughput of the CBS (t/h).

$$Q = 3.6 \times A_{mf} \times V_b \times \rho \tag{5}$$

where A_{mf} is the cross-section area of material flow (m^2) [32,43], ρ is the bulk density of material (kg/m^3) and Q is ton/h in unit.

$$T_{am} = 0.2778 \times Q \times (V_b - V_m) \tag{6}$$

where V_m is the initial velocity of material (m/s) on the belt that was assumed to be 4% of the V_b based on the findings of Doroszuk and Król [45].

Table 1. K_y values based on belt geometry (Modified after [32]).

	Belt slope, δ (°)				
L (m)	0	5	7	14	18
15	0.044	0.044	0.042	0.031	0.027
30	0.040	0.040	0.036	0.027	0.025
76	0.035	0.033	0.031	0.025	0.022
122	0.035	0.029	0.027	0.022	0.020
152	0.034	0.027	0.025	0.020	0.019
244	0.034	0.021	0.020	0.018	0.018
305	0.031	0.019	0.018	0.016	0.016
427	0.029	0.017	0.017	0.016	0.016
610	0.025	0.016	0.016	0.016	0.016

Note: *Interpolation methods can be carried out for various L and a values given above.*

Table 2. Theoretical resistance forces on pulleys (T_{pe}) (Modified after [32]).

Type of pulley	Location of pulley	Wrap angle, θ (°)	T_{pe} (N/pulley)
Driving (motorised)	Tight side	≤ 240	800–1000
Driving and driven	Slack side		500–700
Driven	All other pulleys (bend, snub, and support pulleys)		100–400

The T_{ac} includes the sum of other resistance forces (N) deriving from accessories that include scrapers, belt cleaners, diagonal ploughs, etc. For practical evaluations, T_{ac} can be regarded as a function of the W and W_b. From this point of view, T_{ac} can be quantified by the following equation:

$$T_{ac} = 3 \times W \times W_b \times g \tag{7}$$

where W is the belt width (m).

For the calculation of P_c by the updated version of $CEMA_7$ [41], the online calculation system (version 5.37) of Rulmeca, an international manufacturer of idlers, motorised pulleys, and other components for the bulk handling industry, was used with permission (RCS; https://rcs.rulmeca.com, accessed on 9/11 – 16/2020).

2.2. DIN method

The method of DIN 22,101 [42] has classified the resistance forces acting on CBSs such as primary (F_H), secondary (F_N), gradient (F_{ST}), and special (F_S) ones. Therefore, the sum of these forces determines the T_b (Eq. 8).

$$T_b = F_H + F_N + F_{ST} + F_S \tag{8}$$

The F_H covers the frictional resistance of idlers, belts, and conveyed material. The F_N identifies the frictional resistances arising from contact and acceleration forces between the material and the belt at the feeding point. On the other hand, the F_{ST} and F_S are the gradient and special resistance forces, respectively. The resistance forces described in Eq. 8 were determined by the following equations:

$$F_H = f_c \times L \times g \times [W_{id} + (W_b + W_m)] \times \cos\delta \tag{9}$$

where f_c is the friction coefficient ranging from 0.010 to 0.040. In most cases, the f_c is assumed to be 0.020. W_{id} is the length-related weights (kg/m) of idlers and δ is the belt slope (°).

$$F_N = F_{AUF} + F_{SCH} + F_{GR} \tag{10}$$

where F_{AUF} is similar to the T_{am} (Eq. 6). F_{SCH} is the frictional force between the conveyed material and the feeding chute (Eqs. 11–14), and F_{GR} is the frictional resistance resulting from accessories (Eq. 15).

$$F_{SCH} = C_{rank} \times \left[\frac{I_m}{(V_b + V_m) \times \rho} - \left({b_{sch}}^2 - {l_{ci}}^2\right) \times \frac{\tan(\lambda)}{4}\right]^2 \times \frac{\rho \times g \times l_b \times \mu_2}{{b_{sch}}^2} \tag{11}$$

where C_{rank} is the Rankine factor (Eq. 12), I_m is the nominal material flow ($I_m(\mathrm{kg/s}) = 0.2778 \times Q(\mathrm{t/h})$). b_{sch} is the clear width between materials and feeding chutes (m) (Eq. 13). λ is the through angle of idlers. l_{ci} and l_b are the lengths of the centre carrying idler (m) and the feeding zone (m) (Eq. 14), respectively. μ_2 is the friction coefficient between material conveyed and lateral feeding chutes that can be regarded as 0.6 for most cases.

$$C_{rank} = \tan^2\left(\frac{\pi}{4} - \frac{\beta}{2}\right) \tag{12}$$

where β is the surcharge angle of material flow (°).

For CBSs, whose material flow is greater than 50% of its designed capacity, b_{sch} can be calculated by Eq. 13 as follows:

$$b_{sch} = \frac{l_{ci} \times (1 + \tan(\lambda))}{\tan(\lambda)} \tag{13}$$

$$l_b = \frac{{V_b}^2 - {V_m}^2}{2 \times g \times \mu_1} \tag{14}$$

where μ_1 is the frictional coefficient between the conveyed material and the belt (μ_1 = 0.5–0.7).

$$F_{GR} = \mu_4 \times P_{GR} \times A_{GR} \tag{15}$$

where μ_4 is the friction coefficient between the belt and cleaner (μ_4 = 0.5–0.7), P_{GR} is the dynamic pressure between belt cleaner and belt (P_{GR} = 0.03–0.1 N/mm^2), and A_{GR} is the efficient contact area between belt cleaner and belt (mm^2).

$$F_{st} = H \times g \times (W_b + W_m) \tag{16}$$

where H is metre in unit. W_b and W_m are kg/m in unit. g = 9.81 m/s^2.

Within the context of F_S, the camber resistance force (F_{rst}, N) becomes prominent that was determined by the following equations:

$$F_{rst} = \frac{z_{rst}}{z_r} \times L \times C_{rst} \times \mu_3 \times |\sin \varepsilon_1| \times \cos \delta \times g \times (W_b + W_m) \tag{17}$$

where z_{rst} is the number of carrying idlers set at tilting in one part section, z_r is the total number of carrying idlers in one part section. C_{rst} is the coefficient for calculating chamber resistance (Eq. 18). μ_3 is the friction coefficient between the belt and carrying idlers (μ_3 = 0.5–0.7). ε_1 is the tilt angle of the carrying idlers (ε_1 = 0.5–2 °).

$$C_{rst} = 0.049 \times \lambda^{0.614} \tag{18}$$

Based on the equations mentioned above (Eqs. 8–18), the T_b was calculated, and the P_c was determined using Eq 1 for the DIN method for each CBS.

2.3. DUNLOP–FENNER method

Dunlop–Fenner [43] proposed two practical methods to calculate the P_c, in which the variables of L, Q, V_b, and the sum of the length-related weight of belt and idlers ($W_{b\text{-}id}$, kg/m) were considered. On the other hand, the friction forces deriving from accessories were not integrated into this method's calculations. In this regard, the P_c for this method was calculated by the following equations:

$$P_c = \frac{f_c \times (L + t_f) \times (Q + 3.6 \times W_{b-id} \times V_b)}{367} \pm \frac{Q \times H}{367} \tag{19}$$

where f_c is the general friction factor (For horizontal and inclined CBSs, f_c = 0.0225 and for downhill CBSs, f_c = 0.0135). t_f is the terminal friction constant (Table 3). $W_{b\text{-}id}$ is the total weight of the belt and idlers (Eq. 20).

$$W_{b-id} = 2 \times W_b + \overbrace{\frac{W_{ci}}{S_{ci}} + \frac{W_{ri}}{S_{ri}}}^{W_{id}} \tag{20}$$

Table 3. Terminal friction constant based on belt length [43].

L (m)	t_f (m)
≤ 300	60
300–1200	45
1200–1800	30
≥ 1800	can be neglected

where W_{ci} and W_{ri} are the weights of carrying and return idler sets (kg), $S_{ci,}$ and S_{ri} are the spacings of carrying and return idlers, respectively.

The second method of Dunlop – Fenner (2009) to calculate the P_c is similar to Eq. 19 with several separate parts regarding the loading and unloading conditions of CBS (Eq. 21).

$$P_c = \overbrace{\left(\left(f_e \times \left(L + t_f\right) \times W_{b-id} + f_l \times \left(L + t_f\right) \times \frac{Q}{3.6 \times V_b} \pm \frac{Q \times H}{3.6 \times V_b}\right) \times g \times 10^{-3}\right)}^{T_b} \times V_b \quad (21)$$

where f_e is the friction factor under unloading conditions (f_e = 0.020 for horizontal and inclined CBS and f_e = 0.010 for downhill CBS) and f_l is the friction factor under loading conditions (f_l = 0.025 for horizontal and inclined CBS and f_l = 0.017 for downhill conditions).

It should be noted that Eq. 19 does not include dimensional analysis, it only considers the variables with defined units. The P_c values obtained from Eq. 19 and Eq. 21 were considered together, and the average values obtained from those were presented as the P_c for the Dunlop–Fenner method.

2.4. Field measurements

Field measurements were performed on 43 different CBSs operating in several mining companies in Turkey. Some of the CBSs considered in this study are given as case studies in Figure 2. For each CBS, the current (I, A) drawn by the motorised pulley was measured using a clamp metre (UT204A; 10 Hz–10 MHz, 600 ± 5 V and 400 ± 5A).

Figure 2. Various CBSs considered in this study.

Throughout three complete cycles of belt rotation, the average current (I_{ave}, A) drawn by the CBS was determined under the condition that the Q was greater than 60% of the designed capacity (Figure 3).

Until the desired Q (i.e. the point where $A_{mf}/A_t \geq 0.60$) was reached, the current measurements were monitored, but not recorded. Following this purpose, CBSs were loaded desirably, and the current measurements were then performed systematically. The loaded capacity of CBS was based on the A_{mf} (Figure 1), which was calculated using the procedures of $CEMA_5$ [32] and DIN 22,101 [42]. In this way, the declaration of A_{mf} (Figure 3) was based on the average values obtained from the above–mentioned methods.

The Q for each CBS was calculated using Eq 5. The V_b was measured using a stopwatch, observing the belt's material flow of one complete material transportation. Based on these considerations, the P_c was calculated using Eq 22.

$$P_c = \sum_{i=1}^{n_{mp}} \left(\frac{I_{ave} \times V_n \times PF}{10^3} \right) \tag{22}$$

where I_{ave} is the average current drawn by the CBS, V_n is the nominal voltage (i.e. V_n = 380 volts for most cases), PF is the power factor of the electric motor (PF = 0.80–0.95). n_{mp} is the number of motorised pulleys operating.

During the field measurements, several operational features were also collected (Table 4) and divided into five different groups: belt, material, idler, pulley, and engine properties. These subgroups included quantitative data for the evaluation of P_c.

Owing to the lack of quantitative data on the accessories in/on the CBSs, they were not considered in the analyses. In short, using the variables in Table 4, conventional, statistical, and machine learning methods were carried to estimate the P_c.

2.5. Statistical and machine learning methods

Because of the inability of the conventional methods to capture all parameters influencing the P_c, new techniques were developed for partial or whole-system analysis. Based on the modernisation and development in the CBS technology, such important models are introduced in the following sub-sections.

2.5.1. Multiple linear regression (MLR) analyses

The MLR model has been widely used to define a relationship between dependent and independent variables. The general form of the MLR model is expressed in Eq. (23).

$$f(y) = \alpha_0 + \alpha_1 x_1 + \alpha_2 x_2 \ldots + \alpha_n x_n \tag{23}$$

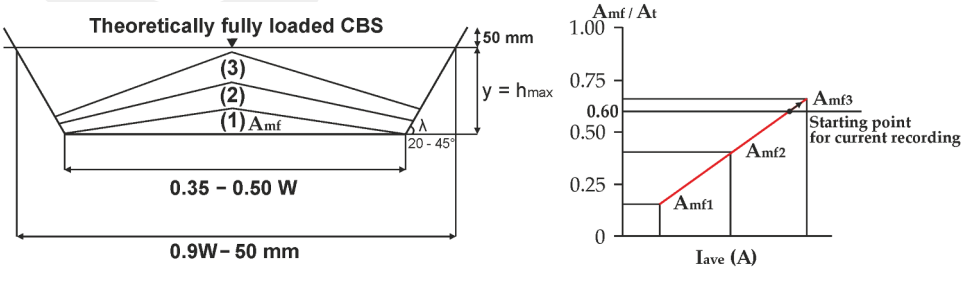

Figure 3. Simplified illustration of the determination of starting point for the current recording (Modified after DIN 22,101 (2002), The figure is not to scale).

Table 4. Operational variables collected during the field measurements.

Variable		Abbreviation	Unit
Belt properties	Belt length	L	m
	Belt width	W	mm
	Belt slope	δ	degree
	Belt speed	V_b	m/s
	Length-related belt weight	W_b [a]	kg/m
Material properties	Bulk density	ρ	kg/m^3
	Surcharge angle	β	degree
	Maximum lump size	S_{max}	mm
	Throughput	Q [b]	t/h
	Length-related material weight	W_m	kg/m
Idler properties	Spacing of carrying idler in one part section	S_{ci}	m
	Spacing of return idler in one part section	S_{ri}	m
	Number of carrying idler in one part section	n_{ci}	–
	Number of return idler in one part section	n_{ri}	–
	Length-related idler weight	W_{id} [c]	kg/m
	Diameter of idlers	D_{id}	mm
	Trough angle	λ	degree
Pulley properties	Number of driven pulleys	n_{dp}	–
	Number of motorised pulleys	n_{mp}	–
	Diameter of motorised pulleys	D_{mp}	mm
Engine properties	Power consumption under operation	P_c	kW
	Installed power	P_{inst}	kW

[a]The Wb is changeable depending upon the belt thickness, number of plies, and strength.
[b]The Q was calculated using Eq. 5.
[c]The Wid is the sum of the weight of carrying and return idlers in one part section.

where y is the dependent variable, x_1 to x_n are the independent variable, α_0 is the constant of the equation, and α_1 to α_n are the coefficients associated with the independent variables listed in Table 4. Adopting the general form of Eq. (23), several models were established, and statistically significant ones were proposed to predict the P_c.

2.5.2. Nonlinear regression (NLR) analyses

For complex problems with a wide range of independent variables, the NLR can also be considered [46]. The typical form of the NLR model adopted in this study is given in Eq. 24. To implement the Eq. 24 for any dataset, it should be linearised, such as given in Eq. 25.

$$f(y) = \alpha_0 \times {x_1}^{\alpha_1} \times {x_2}^{\alpha_2} \ldots \times {x_n}^{\alpha_n} \tag{24}$$

$$\ln(f(y)) = \ln(\alpha_0) + \alpha_1 \ln(x_1) + \alpha_2 \ln(x_2) \ldots + \alpha_n (\ln x_n) \tag{25}$$

Concerning the number of independent variables in conjunction with their relativeness, several linear equation systems were developed. Based on the least-squares approximation, the linear equation systems were solved using the Cholesky Decomposition method. In the NLR analysis context, three or more independent variables (Table 4) were considered in a single run, and the best NLR model was determined statistically.

2.5.3. Gene expression programming (GEP)

The GEP is an evolutionary-based algorithm capable of producing an explicit mathematical formula relating to dependent and independent variables. It originated from genetic programming algorithms [47,48]. In the context of GEP, the chromosome consists of one or more genes encoding smaller subprograms [49].

The gene itself is a fixed-length string composed of various functions and terminals. The head and tail are the two divisions of the gene in GEP. While the head consists of both functions (min, max, *, /, +) and terminals (c_i, d_i), the tail only consists of the terminals, including constants and independent variables. Like other stochastically-based algorithms, the GEP necessitates an initial

population and then uses several selection methods, mutation, and crossover to evolve the population. Each participant's fitness is evaluated using a pre-defined fitness function (e.g. mean squared error: MSE, root mean square error: RMSE, mean absolute error: MAE, etc.). The GEP has been adopted in various science and engineering fields to solve a wide range of problems. In this regard, a novel application of the GEP model was presented in this study. For this purpose, the GeneXpro software was used in implementing various GEP models. The sub-expression trees (Sub-ETs) of the proposed GEP model is presented in Figure 4.

Prior to the development of GEP models, the independent variables should be normalised using Eq 26 to avoid bias in the datasets

$$^{n}P = \frac{P - P_{\min}}{P_{\max} - P_{\min}} \tag{26}$$

where ^{n}P is the normalised parameter, P is the raw value of the parameter, P_{max} and P_{min} are the maximum and minimum value of the P (Table 5), respectively.

In the GEP models, the number of chromosomes, head sizes, tail sizes, and genes were set to 30, 10, 11, and 12, respectively. The linking and fitness functions were multiplication and the root means square error (RMSE), respectively. Based on the optimal strategy for GEP models, the genetic operators were chosen together with the default values of the parameters such as mutation, gene transportation, gene recombination, inversion, etc. The stopping criteria were set to be the maximum fitness. Consequently, the models were run and then stopped when the stopping criteria were reached.

3. Results and discussion

3.1. Effects of operational features on the P_c

The descriptive statistics of the operational features for the investigated CBSs are listed in Table 5. From the descriptive statistics of the variables, one could notice that the CBSs have a wide range of operational features regarding their subgroups. When comparing the P_c values with operational features, it was determined that there are close relationships between the P_c and several operational variables. For instance, when considering the Pearson's correlation coefficient (R) of moderately correlated coupling variables ($R \geq 0.50$ or $R \leq -0.50$), remarkable variables affecting the P_c were determined statistically. Based on the collected data (Table 5), the statistically significant relationships between coupling variables are presented in Table 6.

Regarding the belt properties, as expected, the L, W, V_b, and W_b were statistically significant for the evaluation of P_c. Of the material properties, the Q, irrespective of whether ρ, β, or S_{max}, was the leading parameter. Based on the idler and pulley properties, the W_{id}, n_{dp}, and n_{mp} could be declared other variables that should be considered to evaluate the P_c (Table 6).

Although the δ was found to be negligible with regards to its R-value (R = 0.08), it is indeed a coherent parameter associated with the gradient resistance forces [50]. The underlying reason for obtaining a negligible R-value of δ can be derived from the dataset's monotonicity. More profoundly, most of the CBSs (34/43) had a δ value ranging from – 5° to 5°, which resulted in a relatively low R-value for δ; even so, the δ was regarded as an independent variable for further analyses. In summary, together with the δ, the statistically significant variables written boldly in Table 6 were established to evaluate P_c in this study. These variables were declared crucial independent variables to estimate the P_c.

3.2. Comparison of the P_c values based on the conventional methods

For the purpose of gaining an objective comparison, the relationships between the measured P_c and those obtained from the conventional methods were presented as linear trends without intercept

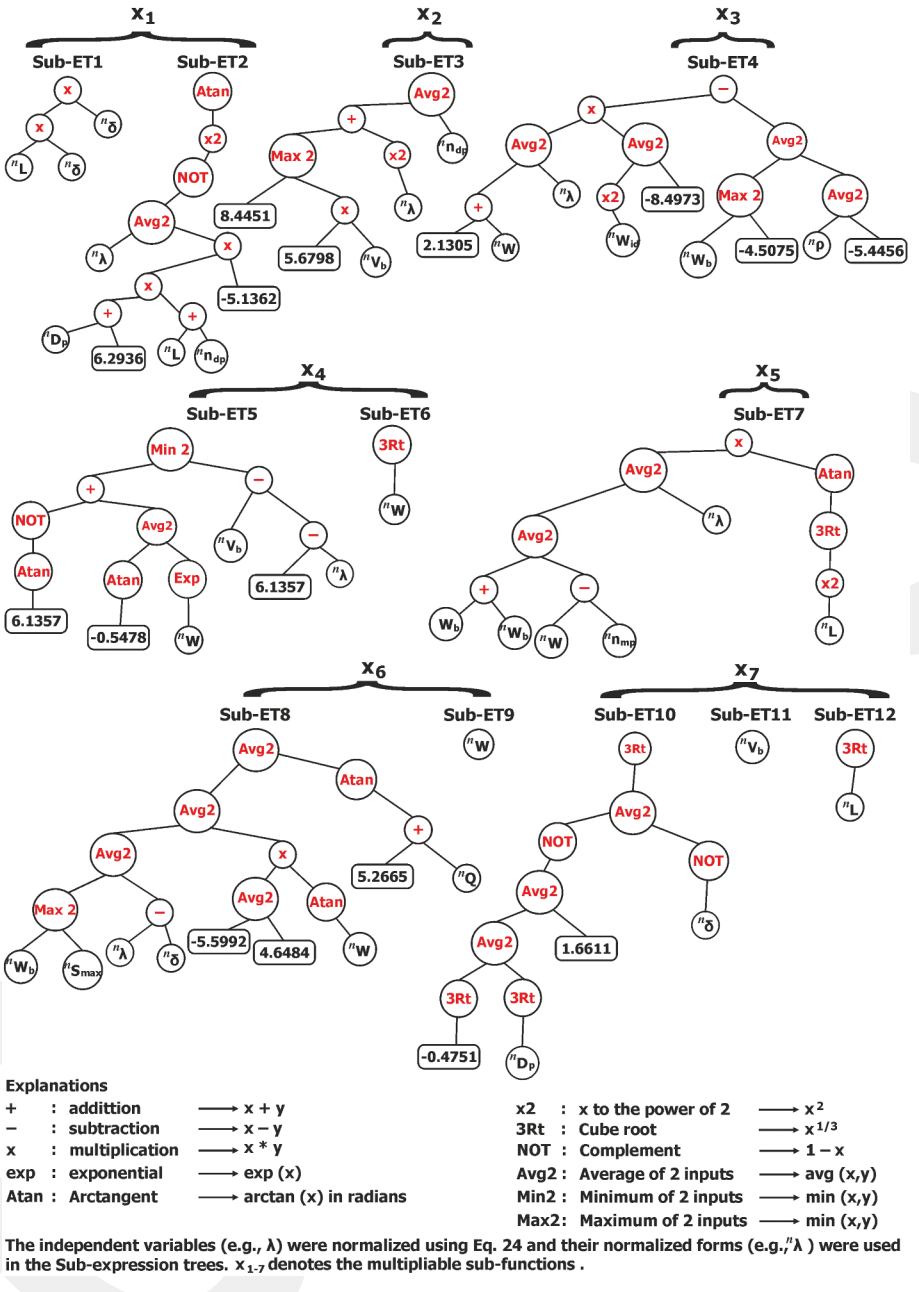

Figure 4. Sub-Expression trees of the proposed GEP model.

$(f(y) = a * x)$ that enabled several convergence factors (CFs) linking to the measured P_c. For different P_c intervals, the linear relationships are illustrated in Figure 5. Adopting different CFs, one can claim that all methods can provide reasonable P_c values for definite CBSs.

The methods of $CEMA_5$, $CEMA_7$, and DIN yielded a correlation of determination (R^2) greater than 0.93. For the referred methods, the CFs were found to be 0.709 ± 0.016, 0.882 ± 0.020 and 0.98 ± 0.021, respectively. Of the conventional methods, the lowest R^2 was found for the Dunlop–Fenner method with an R^2 of 0.83. The CF for this method was 1.009 ± 0.039.

Table 5. Descriptive statistics of the variables considered in this study.

Belt properties	Min	Mean	Max	Std. dev.	Cov (%)	Q_1	Q_2	Q_3
L (m)	7.00	73.33	230.00	56.62	77	32.00	50.00	114.00
W (mm)	400.00	895.30	1200.00	203.50	23	800.00	900.00	1000.00
δ (°)	–4.00	4.49	23.57	6.50	145	0.00	2.87	5.33
V_b (m/s)	0.23	1.49	3.21	0.78	52	0.89	1.44	2.04
W_b (kg/m)	5.00	17.71	35.00	6.72	38	13.00	17.00	22.00
Material properties	Min	Mean	Max	Std. dev.	Cov (%)	Q_1	Q_2	Q_3
ρ (kg/m^3)	1125.00	1584.80	2240.00	251.70	16	1400.00	1540.00	1710.00
β (°)	10.00	15.97	25.00	4.02	25	15.00	15.00	18.00
S_{max} (mm)	25.00	125.80	300.00	68.30	54	75.00	110.00	160.00
Q (t/h)	28.00	72.30	2030.00	473.90	655	299.00	560.00	1051.00
W_m (kg/m)	20.37	120.18	238.60	55.36	46	81.81	116.86	160.27
Idler properties	Min	Mean	Max	Std. dev.	Cov (%)	Q_1	Q_2	Q_3
S_{ci} (m)	1.00	1.44	2.00	0.23	16	1.30	1.50	1.50
S_{ri} (m)	1.50	2.81	4.00	0.54	19	2.50	3.00	3.00
n_{ci}	2.00	2.93	5.00	0.59	20	3.00	3.00	3.00
n_{ri}	1.00	1.14	2.00	0.35	31	1.00	1.00	1.00
W_{id} (kg/m)	1.53	13.70	33.30	7.10	52	9.01	13.31	16.53
D_{id} (mm)	108.00	123.77	159.00	25.34	20	108.00	127.00	133.00
λ (°)	10.00	34.72	45.00	8.47	24	35.00	35.00	40.00
Pulley properties	Min	Mean	Max	Std. dev.	Cov (%)	Q_1	Q_2	Q_3
n_{dp}	1.00	2.98	6.00	1.41	47	2.00	3.00	4.00
n_{mp}	1.00	1.39	2.00	0.49	35	1.00	1.00	2.00
D_p (mm)	250.00	484.10	800.00	187.80	39	315.00	500.00	630.00
Engine properties	Min	Mean	Max	Std. dev.	Cov (%)	Q_1	Q_2	Q_3
P_c (kW)	0.23	15.33	44.94	12.32	80	3.62	13.10	25.20
P_{inst} (kW)	0.25	20.03	60.00	15.07	75	5.50	18.40	30.00

Min: Minimum value, Mean: Average value, Max: Maximum value, Std. Dev.: Standard deviation, Cov: Coefficient of variation, Q_1: Lower quartile (25%), Q_2: Median, Q_3: Upper Quartile (75%).

Table 6. Pearson's correlation matrices of the variables considered in this study.

Belt properties

Variable	L (mm)	W (mm)	δ (°)	V_b (kg/m)	W_b (kg/m)	P_c (kW)
L (mm)	1					
W (mm)	0.15	1				
δ (°)	–0.43	–0.03	1			
V_b (m/s)	0.61	0.39	–0.28	1		
W_b (kg/m)	0.14	0.83	0.06	0.47	1	
P_c (kW)	**0.54**	**0.52**	0.08	**0.74**	**0.61**	1

Material properties

Variable	ρ (kg/m^3)	β (°)	S_{max} (mm)	Q (t/h)	W_m (kg/m)	P_c (kW)
ρ (kg/m^3)	1					
β (°)	–0.41	1				
S_{max} (mm)	0.12	0.01	1			
Q (t/h)	–0.19	0.12	0.17	1		
W_m (kg/m)	0.04	0.09	0.32	0.69	1	
P_c (kW)	–0.18	0.05	0.03	**0.82**	0.47	1

Idler properties

Variable	S_{ci} (m)	S_{ri} (m)	n_{ci}	n_{ri}	W_{id} (kg/m)	D_{id} (mm)	λ (°)	P_c (kW)
S_{ci} (m)	1							
S_{ri} (m)	0.67	1						
n_{ci}	–0.03	–0.18	1					
n_{ri}	0.13	0.23	0.28	1				
W_{id} (kg/m)	–0.44	–0.31	–0.17	0.02	1			
D_{id} (mm)	0.01	0.10	–0.47	–0.07	0.75	1		
λ (°)	0.02	–0.22	0.15	0.01	0.09	0.08	1	
P_c (kW)	–0.23	–0.14	–0.08	0.20	**0.55**	0.32	0.05	1

Pulley properties

Variable	n_{dp}	n_{mp}	D_p (mm)	P_c (kW)
n_{dp}	1			
n_{mp}	0.36	1		
D_p (mm)	0.41	0.32	1	
P_c (kW)	**0.50**	**0.62**	0.42	1

Engine properties

Variable	P_{inst} (kW)	Pc (kW)
P_{inst} (kW)	1	
P_c (kW)	**0.99**	1

** The bolded values (e.g. **0.74**) indicate the statistically significant variables for the evaluation of P_c.*

Focusing on the CFs as a relative measure of predicting the P_c, on average rates, the methods of $CEMA_5$ and $CEMA_7$ overestimated the measured P_c approximately by 29% and 12%, respectively (Figure 5a, 5b). Various researchers also obtained similar overestimations using the CEMA methods. For a 6.1 km length CBS, the actual P_c was overestimated by up to 70%, considering the method $CEMA_5$ [51]. Satria and Rusli [52] found that the method of $CEMA_5$ overestimated the P_c of a 154 m length CBS from a range of 10% to 46%, compared to those obtained from the methods of $CEMA_6$ and DIN 22,101, respectively.

Contrary to the CEMA methods, the DIN 22,101 was found to be the most convenient method for the CBSs investigated in this study. In this regard, the method overestimated the measured P_c values by only 2%, on average (Figure 5c). Of the conventional methods, the Dunlop–Fenner presented the minor performance (Figure 5d) owing to their undulating calculations, especially for downhill and relatively higher inclined ($\delta > 15–20°$) CBSs.

In general, excluding the accessories in/on CBSs, all variables/components (Table 4) were considered and integrated into the conventional methods. Therefore, it could be claimed that the relative success of the conventional methods in predicting the P_c was derived from the data collection methodology and performing direct measurements on the P_c. Since most CBSs spend a

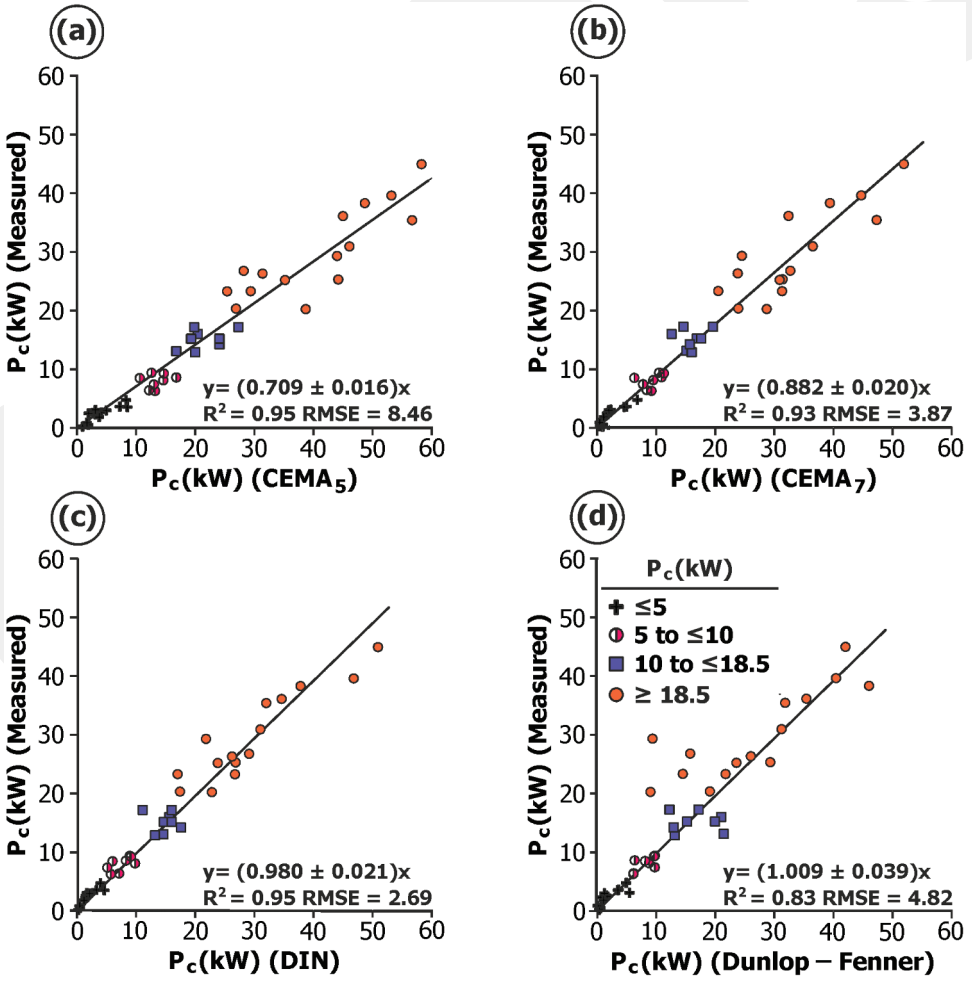

Figure 5. Linear relationships between the measured and obtained P_t values from conventional methods a) $CEMA_5$ b) $CEMA_7$ c) DIN d) Dunlop – Fenner.

Table 7. The variations in the CFs.

Methods	Average CF	Upper bound	Lower bound	R^2	RMSE	Average global deviation, AGD
$CEMA_5$	0.709	0.741	0.677	0.95	8.46	64
$CEMA_7$	0.882	0.922	0.842	0.94	3.87	27
DIN[a]	**0.980**	**1.058**	**0.941**	**0.95**	**2.69**	**17**
Dunlop–Fenner	1.009	1.051	0.967	0.83	4.82	23
MLR	1.001	1.081	0.921	0.84	4.88	110
NLR[a,b]	**1.005**	**1.053**	**0.957**	**0.94**	**2.99**	**20**
GEP[b]	**1.027**	**1.075**	**0.979**	**0.94**	**2.96**	**28**

[a]Recommended method for the design of P_t in for the TMI
[b]Recommended methods for the optimisation of the P_c for the TMI
Note: P_{inst} = 1.3–1.5P_c in this study. $AGD = \frac{100}{n}\sum_{i=1}^{n}\left|\left(\frac{y_{est}-y_{meas.}}{y_{meas}}\right)\right|$

considerable part of the total energy under unloading conditions [50], the average loading rate of 75% (See *Engine properties* in Table 5) caused reasonable correlations between theoretical calculations and practical measurements. The substantial impacts of the belt conveyor loading rate on the performance of CBSs elements [53] also revealed the performance of the motorised head pulleys. Otherwise, there would be remarkable changes in the estimated P_c values. Specific to the methods, both the $CEMA_{5,7}$ and DIN 22,101 can be reliably utilised to predict the P_c for the investigated CBSs, providing that the CFs (Table 7) are adopted.

Nevertheless, the DIN 22,101 might take the lead owing to its overall success (R^2 = 0.95) and the CF, which is nearer to 1 (Figure 5c). Despite the performances of the traditional methods, they have inherent drawbacks, which are time-consuming calculation processes. Therefore, it is imperative to develop alternative robust models that are adaptive, user-friendly, and can account for all effective parameters simultaneously regarded in power calculations of CBSs. Such important models are proposed in the following sub-section.

3.3. Comparison of the P_c values based on statistical and machine learning methods

Using statistical and machine learning methods described in Section 2.5, remarkable relationships were obtained to estimate the P_c. Based on the MLR and NLR analysis results, the P_c can be estimated by the following equations (Eqs 27 and 28).

For the MLR model;

$$P_c = -6.98 + 0.0912L + 0.702\delta + 0.01849Q, R^2 = 0.77 \tag{27}$$

For the NLR model;

$$P_c = 0.00008 \times L^{0.615} \times (10+\delta)^{1.352} \times Q^{1.020} \times (W_b + W_{id})^{-0.178}, R^2 = 0.94 \tag{28}$$

In these regression models, the most important independent variables affecting the P_c were benefited. Given the dataset (Table 5), the Q can also be predicted by considering several properties such as W, V_b, n_{mp}, q, and β (Eq. 29).

$$Q = -2189 + 1.088W + 364.7V_b + 177.9n_{mp} + 0.465\rho + 22.58\beta, R^2 = 0.91 \tag{29}$$

Nevertheless, an empirical formula was also established for the GEP method by simplifying and merging some of the Sub-ETs in Figure 4. Adopting the multipliable sub-fuctions (i.e. x_{1-7}) of the GEP, the P_c can also be estimated the following equations:

$$P_c = 44.7108\prod_{i=1}^{7} x_i + 0.228 \tag{30}$$

$$x_1 = {}^{n}L\,{}^{n}\delta^2 \tan^{-1}\left[\left\{1 - 0.5\left({}^{n}\lambda - 5.1362\left({}^{n}D_p + 6.2936\right)\left({}^{n}L + {}^{n}n_{ndp}\right)\right)\right\}^2\right] \tag{31}$$

$$x_2 = 0.5\left[\max\left(8.4451; 5.6798\,{}^{n}V_b\right) + {}^{n}\lambda^2 + {}^{n}n_{dp}\right] \tag{32}$$

$$x_3 = 0.25\left(2.1305 + {}^{n}W + {}^{n}\lambda\right)\left({}^{n}w_{id}^2 - 8.4973\right) - 0.5\max\left({}^{n}W_b; -4.5075\right) - 0.25\left({}^{n}\rho - 5.4456\right) \tag{33}$$

$$x_4 = {}^{n}W^{1/3} \times \min\left[\left\{-0.4092 + 0.5\left(-0.5012 + e^{{}^{n}W}\right)\right\}, \left({}^{n}V_b - 6.1357 + {}^{n}\lambda\right)\right] \tag{34}$$

$$x_5 = 1 - 0.5\left[0.5\left(2\,{}^{n}W_b + {}^{n}W - {}^{n}n_{mp}\right) + \lambda\right]\tan^{-1}\left({}^{n}L^{2/3}\right) \tag{35}$$

$$x_6 = 0.5\left[0.25\left(\max\left({}^{n}w_b; {}^{n}S_{\max}\right) + {}^{n}\lambda - {}^{n}\delta\right) - 0.2377\tan^{-1}\left({}^{n}W\right) + \tan^{-1}\left(5.2666 + {}^{n}Q\right)\right] \times {}^{n}W \tag{36}$$

$$x_7 = \left[0.5\left(0.3645 - 0.25\,{}^{n}D_p^{1/3} + 1 - {}^{n}\delta\right)\right]^{1/3} {}^{n}V_b \times {}^{n}L^{1/3} \tag{37}$$

where x_{1-7} are the numerical sub-functions depicted as the Sub-ETs in Figure 4.

By employing the above-mentioned equations (Eqs. 27–37), the P_c was estimated for the investigated CBSs, and the results were compared with the ones measured. Despite its relatively promising $R^{2,}$ the MLR method did not yield consistent P_c values, particularly for the CBSs operating below 30 kW (Figure 6a). However, the NLR (Figure 6b) and GEP (Figure 6c) models turned out to be good alternatives in estimating the P_c. For the NLR and GEP models, the CFs were found to be 1.005 ± 0.024 and 1.027 ± 0.024, respectively.

The findings obtained from the statistical and machine learning methods demonstrated that the NLR and GEP could be feasible methods for the evaluation of P_c. In these methods, the essential variables of the CBSs were considered. On this point, the design and optimisation of P_c could be carried out considering these methods.

Notably, it should be mentioned that mining companies, who are willing to construct such conveyor belts, can use the NLR method for conveyor belt design studies. After these CBSs have been installed, the optimisation of P_c can be eligible using the proposed GEP model owing to its dynamic capability. With the use of NLR and GEP models together, a comprehensive conveyor belt design and optimisation package can be introduced.

3.4. Concluding remarks

The comparisons based on the measured and estimated P_c values indicated that the applied methods, excluding the Dunlop–Fenner, and MLR, have no distinct superiority in predicting the P_c. For design studies, the CEMA methods, DIN, and NLR could be utilised to estimate the P_c. Since the GEP requires a dataset before the calculation process, it is not appropriate to design studies. It is rather than suitable for the optimisation of P_c for CBSs under working conditions. By collecting field data, the GEP could be easily implemented for such optimisation studies. The GEP can also have such flexibilities for analysing subsystems of CBSs that can be declared another advantage. Based on the additional analyses covering the deviation of the estimated P_c values, the performance of the methods was also examined. Of the conventional methods, it was determined that the DIN could be declared the most convenient method for the investigated CBSs with the lowest average global deviation (AGD) of 17. On the other hand, the NLR and GEP could be other alternatives when considering the AGD that ranges from 20 to 28 (Table 7). In any case regarding conservative

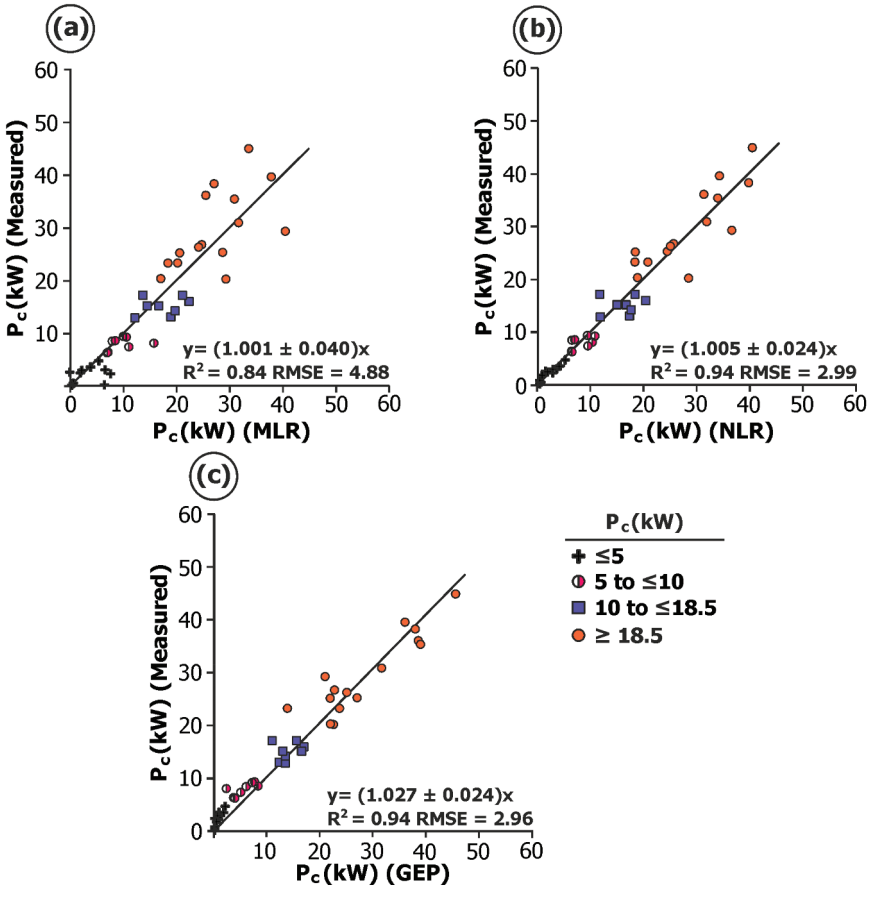

Figure 6. Linear relationships between the measured and obtained P_t values from statistical and machine learning methods a) MLR b) NLR c) GEP.

approaches, it is recommended to use the upper bound CFs in Table 7 to evaluate either the P_c or P_{inst}.

One of the present study's core findings is the determination of variables affecting the P_c (Table 6). Although they are well-known parameters for material transportation science and technology, their significance level was uncovered statistically and validated in this study. Thanks to these variables, remarkable empirical formulae were constructed based on the NLR and GEP models. Besides, several CFs were also determined that made such comparisons possible to evaluate the P_c. It is worth reminding that the use of CFs could have some limitations for such CBSs beyond the present study. When it comes to the criticism of the methods, it was concluded that several undulating/inconsistent results were obtained for the CBSs operating below 18.5 kW (Fig 5, 6).

These results were almost obtained for downhill and relatively inclined CBSs ($\delta > 15°–20$). For these CBSs, further studies are required within the concepts of both conventional and other numerical-based methods.

Apart from the issues related to design and optimisation proposals, apparent similarities and differences were also observed in the operational features of the CBSs. The variations in the D_p are given in Figure 7a. It is clear from the figure that no standardised D_p values conform to definite belt geometries. However, for the sake of a generalised idea, it can be claimed that the D_p should increase with increasing the W of CBSs. In another respect, it was observed that most of the CBSs with $P_{inst} \geq$

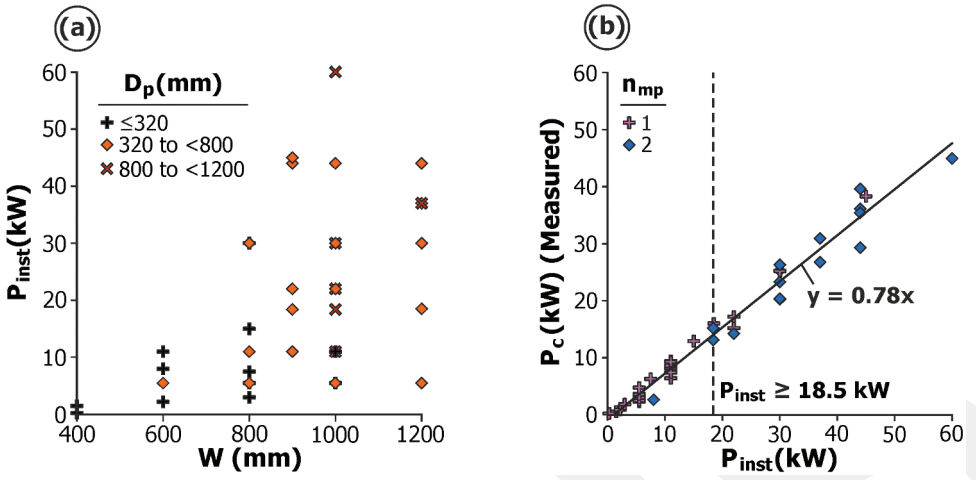

Figure 7. Evaluation of the CBSs regarding several operational features a) Variations in the D_p due to W b) Variations in the n_{mp} due to $P_{inst.}$

18.5 kW are operated by dual drives (n_{mp} = 2). In other words, the CBSs operating below 18.5 kW generally use single drives (n_{mp} = 1) (Figure 7b).

Moreover, during the field measurements, it was observed that no drive-control systems or soft starters were used/adapted to the investigated CBSs. However, the P_c can be diminished by using such kind of drive-control systems. Since the installation, operation, and maintenance costs of CBSs are less than their initial investment, cost-saving infrastructures and attempts to increase the system life should be considered [54]. From these perspectives, the fact remains that conventional methods for CBSs seem hard to optimise and analyse subsystems due to their complicated structures, lack of dynamic adaption, and long-lasting calculation steps. At this stage, the NLR and GEP models with several modifications can analyse several CBS infrastructures. These models are relatively easy and capable of dynamic calculations. In this respect, the present study could be declared a case study noted for combining theoretical and practical approaches to power calculation methodologies for CBSs used in several mining applications.

4. Conclusions

The present study encompasses field data of several CBSs that were used in the TMI. These CBSs are mainly utilised to transport materials either broken by crushers or discharged by silos and bypass systems. The primary purpose of the study is to investigate the P_c of these CBSs through different methods. The actual P_c of the CBSs was measured directly on motorised head-pulleys. During the field measurements, quantitative data on operational features were collected for each CBS. Then, the P_c was calculated for each CBS using the methods of $CEMA_{5-7}$, DIN 22,101 and Dunlop–Fenner. Excluding the Dunlop–Fenner method, all conventional methods could be applicable for the evaluation of P_c, adopting various CFs (Table 7). In particular, the DIN 22,101 was found to be the most convenient method for the investigated CBSs.

The most significant variables affecting the P_c were determined statistically (Table 6). Using these variables, promising predictive models were established based on the NLR and GEP methods. In the light of the error analyses, it was concluded that the NLR and GEP could be appliable for the evaluation of P_c. Therefore, with or without several modifications, they should be attempted to such CBSs to observe difficulties/similarities of quantifying the P_c. In this way, the actual performance of the developed methods would be examined.

Last but not least, the relative success of implementing both the conventional and modern methods in predicting the P_c also shows a relative measure of the data collection method and treatment of the direct measurements on P_c. For further analyses or field measurements related to the CBSs, it is recommended that the Q should be at least greater than 80% of the designed capacity of CBSs, within the bounds of possibility. In this way, relative errors in measuring and predicting the P_c could be reduced.

Acknowledgments

The authors are greatly indebted to anonymous mining companies who provided their facilities during the field measurements and shared the quantitative data of the investigated CBSs. Special thanks are due to RULMECA, who enabled the corresponding author to use their online calculation system. Last but not least, special thanks are due to the anonymous reviewers and the handling editor for constructive comments and suggestions that improved the study.

Disclosure statement

The authors declare that they have no known competing financial interests or personal relationships that could have influenced the work reported in this paper.

ORCID

Ekin Köken http://orcid.org/0000-0003-0178-329X

References

[1] D. Clenét Optimising energy efficiency of conveyors. Schneider Electric Document Number: WP20100601EN. Rueil Malmaison, France, 2010, 21 pp.
[2] A.W. Roberts and J.W. Hayes, *Economic Analysis in the Optimal Design of Conveyors, Tunra Ltd.*, Univ. Newcastle, Australia, 1979.
[3] H. Lieberwirth, *Economic advantage of belt conveying in open-pit mining*, in *Mining Latin America*, Dordrech: Springer, 1994, 279–295. 978-94-011-1216-1.
[4] U. Köhler, M. Sykulla, and V. Wuschek, *Variable-speed belt conveyors gaining in importance*, Braunkohle Surf. Min. 53 (2001), pp. 65–72.
[5] P. Bindzár and D. Malindžák, *Number of conveyor belts optimization regarding to its type and logistical parameters in mining industry*, Acta Montanistica Slovaca 13 (2008), pp. 524–531.
[6] P.M. Mcguire, *Conveyors: Application, Selection, and Integration*, CRC Press, 2010, 210 pp, 978-1439803882.
[7] S. Zhang and X. Xia, *Modeling and energy efficiency optimization of belt conveyors*, Appl. Energy. 88, 9 (2011), pp. 3061–3071. doi:10.1016/j.apenergy.2011.03.015
[8] T. Braun, A.H. Hennig, and B.G. Lottermoser, *The need for sustainable technology diffusion in mining: Achieving the use of belt conveyor systems in the German hard-rock quarrying industry*, J. Sustain. Min. 16, 1 (2017), pp. 24–30. doi:10.1016/j.jsm.2017.06.003
[9] D. Woźniak, *Laboratory tests of indentation rolling resistance of conveyor belts*, Measurement. 150 (2020), pp. 107065. doi:10.1016/j.measurement.2019.107065
[10] S. Al-Thyabat, N.J. Miles, and T.S. Koh, *Estimation of the size distribution of particles moving on a conveyor belt*, Miner. Eng. 20, 1 (2007), pp. 72–83. doi:10.1016/j.mineng.2006.05.011
[11] R. Schmitz, U. Kübeler, H.J. Perleberg, R. Hempel, and F. Elandaloussi, *Conveyor belt muck built-up detection and messaging system*, Min. Tech. 117, 3 (2008), pp. 111–115. doi:10.1179/174328608X368824
[12] A. Taskinen, M. Vilkko, P. Itävuo, and A. Jaatinen, *Fast Size Distribution Estimation of Crushed Rock Aggregate using Laserprofilometry*, IFAC Proc. 44, 1 (2011), pp. 12132–12137. doi:10.3182/20110828-6-IT-1002.01787
[13] D. Prostański, *Use of air-and-water spraying systems for improving dust control in mines*, J. Sustain. Min. 12, 2 (2013), pp. 29–34. doi:10.7424/jsm130204
[14] A. Niemela, E. Hasikova, and V. Titov, *Real-time material flow analysis on conveyor belts*, IFAC-PapersOnLine. 48, 17 (2015), pp. 24–27. doi:10.1016/j.ifacol.2015.10.071
[15] M. Kontny, *Machine vision methods for estimation of size distribution of aggregate transported on conveyor belts*, Vibroengineering PROCEDIA. 13 (2017), pp. 296–300. doi:10.21595/vp.2017.19151

[16] G.F. Golikov, D.V. Ryabov, S.N. Galashin, and Y. Kondrashin, *A quality control of the joints of fabric rubber conveyor belts with the aid of a thermovisor*, Int. J. Polymer. Sci Tech. 44, 11 (2018), pp. 47–50. doi:10.1177/0307174X1704401110
[17] L. Jurdziak, R. Blazej, and M. Barja, *Conveyor belt 4.0*, in *Intelligent Systems in Production Engineering and Maintenance. ISPEM 2018, Advances in Intelligent Systems and Computing* Vol. 835, A. Burduk, E. Chlebus, T. Nowakowski, and A. Tubis, eds., Springer, Cham, 2019, pp. 645 - 654. doi:10.1007/978-3-319-97490-3_61.
[18] R. Yang, T. Qiao, Y. Pang, Y. Yang, H. Zhang, and G. Yan, *Infrared spectrum analysis method for detection and early warning of longitudinal tear of mine conveyor belt*, Measurement. 165 (2020), pp. 107856. doi:10.1016/j.measurement.2020.107856
[19] V.L. Yakolev, V.A. Bersenev, A.V. Glebov, S.S. Kulniyaz, and M.A. Marinin, *Selecting cyclical-and-continuous process flow diagrams for deep open pit mines*, J. Min. Sci. 55, 5 (2019), pp. 783–788. doi:10.1134/S106273911905615X
[20] A. Middelberg, J. Zhang, and X. Xia, *An optimal control model for load shifting–With application in the energy management of a colliery*, Appl. Energy. 86, 7–8 (2009), pp. 1266–1273. doi:10.1016/j.apenergy.2008.09.011
[21] X. Xia and J. Zhang, *Energy efficiency and control systems–from a POET perspective*, IFAC Proc. 43, 1 (2010), pp. 255–260. doi:10.3182/20100329-3-PT-3006.00047
[22] PCI Conveyor pulley selection guide; 2014, 32 pp. https://www.pcimfg.com/wp-content/uploads/2014/11/PCI_Pulley_Selection_Guide_2014.pdf
[23] G. Lodewijks, *Dynamics of belt systems*, diss., Delft Univ. Tech., Delft; 1996, 276 pp. 90-370-0145-9
[24] X. Liu, *Prediction of belt conveyor idler performance*, diss., Delft Univ. Tech., Delft; 2016, 176 pp.
[25] S. Zhang and X. Xia, *Optimal control of operation efficiency of belt conveyor systems*, Appl. Ener. 87, 6 (2010), pp. 1929–1937. doi:10.1016/j.apenergy.2010.01.006
[26] L. Zhao and Y. Lin, *Typical failure analysis and processing of belt conveyor*, Proc. Eng. 26 (2011), pp. 942–946. doi:10.1016/j.proeng.2011.11.2260
[27] C. Webb, M. Hodkiewicz, N. Khan, R. Wilson, and S. Muller, Conveyor belt wear life modelling, CEED Seminar Proceedings, Univ. Western Austr, Perth; 2013, pp 25–30.
[28] X. Liu, Y. Pang, and G. Lodewijks, *Theoretical and experimental determination of the pressure distribution on a loaded conveyor belt*, Measurement. 77 (2016), pp. 307–316. doi:10.1016/j.measurement.2015.08.041
[29] S.H. Zhou, F. Zeng, J. Du, Q. Wu, and F. Ren Experimental research on the energy consumption laws and its influencing factors of belt conveyor systems. In: 13th Int Comp. Conf. on Wavelet Active Media Tech. Infor. Proc. (ICCWAMTIP), Chengdu; 2016, pp 395–402, doi:10.1109/ICCWAMTIP.2016.8079881
[30] T. Mathaba and X. Xia, *Optimal and energy efficient operation of conveyor belt systems with downhill conveyors*, Energy Effic. 10, 2 (2017), pp. 405–417. doi:10.1007/s12053-016-9461-8
[31] R. Król, W. Kawalec, and L. Gladsiewicz, *An effective belt conveyor for underground ore transportation systems*, IOP Conf. Series: Earth. Environ. Sci. 95 (2017), pp. 042047. doi:10.1088/1755-1315/95/4/042047
[32] *CEMA$_5$ Conveyor Equipment Manufacturers Association Belt Conveyors for Bulk Materials*, 5th, 2002. 1-891171-18-6
[33] Y. Yao and B. Zhang, *Influence of the elastic modulus of a conveyor belt on the power allocation of multi-drive conveyors*, PLoS ONE. 15, 7 (2020), pp. e0235768. doi:10.1371/journal.pone.0235768
[34] R.T. Swinderman and A.J. Waters, Conveyor belt cleaner scraper blade with sensor and control system therefor, United States Patent (No: US008267239B2); 2012, 33 pp.
[35] M.J. Bleau, J.:J. Dellach, and K.P. Dellach, Apparatus for cleaning a conveyor belt, United States Patent (No: US00824046OB1); 2012, 11 pp.
[36] R. Blazej, L. Jurdziak, T. Kozlowski, and A. Kirjanów, *The use of magnetic sensors in monitoring the condition of the core in steel cord conveyor belts–Tests of the measuring probe and the design of the DiagBelt system*, Measurement. 123 (2018), pp. 48–53. doi:10.1016/j.measurement.2018.03.051
[37] L.B. Ristić, M.Z. Bebić, D.S. Jevtić, I.D. Mihailović, S.Ž. Štatkić, N.T. Rašić, and B.I. Jeftenić, Fuzzy speed control of belt conveyor system to improve energy efficiency. In: 15th Int. Power Electr. Mot. Cont. Conf., EPE/ PEMC; 2012, Novi Sad, Serbia. doi:10.1109/EPEPEMC.2012.6397260
[38] Y. Pang, G. Lodewijks, and D.L. Schott, *Fuzzy controlled energy saving solution for large-scale belt conveying systems*, Appl. Mech. Mater. 260–261 (2013), pp. 59–64. 10.4028/www.scientific.net/AMM.260-261.59
[39] L. Petru and G. Mazen, *Experimental stand for the study of a three-phase synchronous generator with permanent super magnets*, Proc. Eng. 69 (2014), pp. 231–236. doi:10.1016/j.proeng.2014.02.226
[40] D. He, Y. Pang, and G. Lodewijks, *Green operations of belt conveyors by means of speed control*, Appl. Ener. 188 (2017), pp. 330–341. doi:10.1016/j.apenergy.2016.12.017
[41] *CEMA$_7$ Conveyor Equipment Manufacturers Association Belt Conveyors for Bulk Materials*, 7th, 2014. 978-1891171-44-4
[42] DIN 22101 German Institute for standardization: Continuous conveyors - Belt conveyors for loose bulk materials - Basis for calculation and dimensioning; 2002, 51 pp.
[43] Dunlop–fenner conveyor handbook: Conveyor belting Australia; 2009, 103 pp.

[44] T. Mathaba and X. Xia, *A parametric energy model for energy management of long belt conveyors*, Energies. 8, 12 (2015), pp. 13590–13608. doi:10.3390/en81212375
[45] B. Doroszuk and R. Król, *Analysis of conveyor belt wear caused by material acceleration in transfer stations*, Min. Sci. 26 (2019), pp. 189–201. doi:10.5277/msc192615
[46] J. Schoukens and L. Ljung, *Nonlinear system identification, A user-oriented roadmap*, IEEE Control Syst Mag 39 (2019), pp. 28–99.
[47] C. Ferreira, *Gene expression programming: A new adaptive algorithm for solving problems*, Complex Syst (2001), pp. 13(2): 87–129.
[48] J. Zhong, L. Feng, and Y.S. Ong, *Gene expression programming: A survey*, IEEE Comput Intell Mag 12 (3) (2017), pp. 54–72. doi:10.1109/MCI.2017.2708618.
[49] A.H. Gandomi and A.H. Alavi, *A new multi-gene genetic programming approach to nonlinear system modeling. Part I: Materials and structural engineering problems*, Neural Comput Appl 21 (1) (2012), pp. 171–187. doi:10.1007/s00521-011-0734-z.
[50] M.A. Alspaugh Latest developments in belt conveyor technology. In: MINExpo, Las Vegas, NV, USA; 2004.
[51] G. Lodewijks and D.J. Kruse, *The power of field measurements–part I*, Bulk Solids Handling 18 (1998), pp. 415–427.
[52] I. Satria and M. Rusli, *A comparison of effective tension calculation for design Belt conveyor between CEMA and DIN Standard*, MATEC Web Conf. 166 (2018), pp. 01007. doi:10.1051/matecconf/201816601007
[53] R. Król, W. Kisielewski, D. Kaszuba, and L. Gladysiewicz, *Testing belt conveyor resistance to motion in underground mine conditions*, Int. J. Min. Rec. Environ. 31, 1 (2016), pp. 78–90. doi:10.1080/17480930.2016.1187967
[54] T. Mushiri and C. Mbohwa, "Design of a Power Saving Industrial Conveyor System," Lecture Notes in Engineering and Computer Science: Proceedings of The World Congress on Engineering and Computer Science 2016, 19–21 October, 2016, San Francisco, USA, pp 942–947